

# Photoelectron spectroscopy with Octopus

**Umberto De Giovannini**

University of the Basque Country,

San Sebastian, Spain

[umberto.degiovannini@ehu.es](mailto:umberto.degiovannini@ehu.es)



Universidad  
del País Vasco

Euskal Herriko  
Unibertsitatea



# Outline

- Overview:

**Photoelectron Spectroscopy**

- The Method:

**Modeling photoelectrons**

**The Mask Method + Octopus implementation**

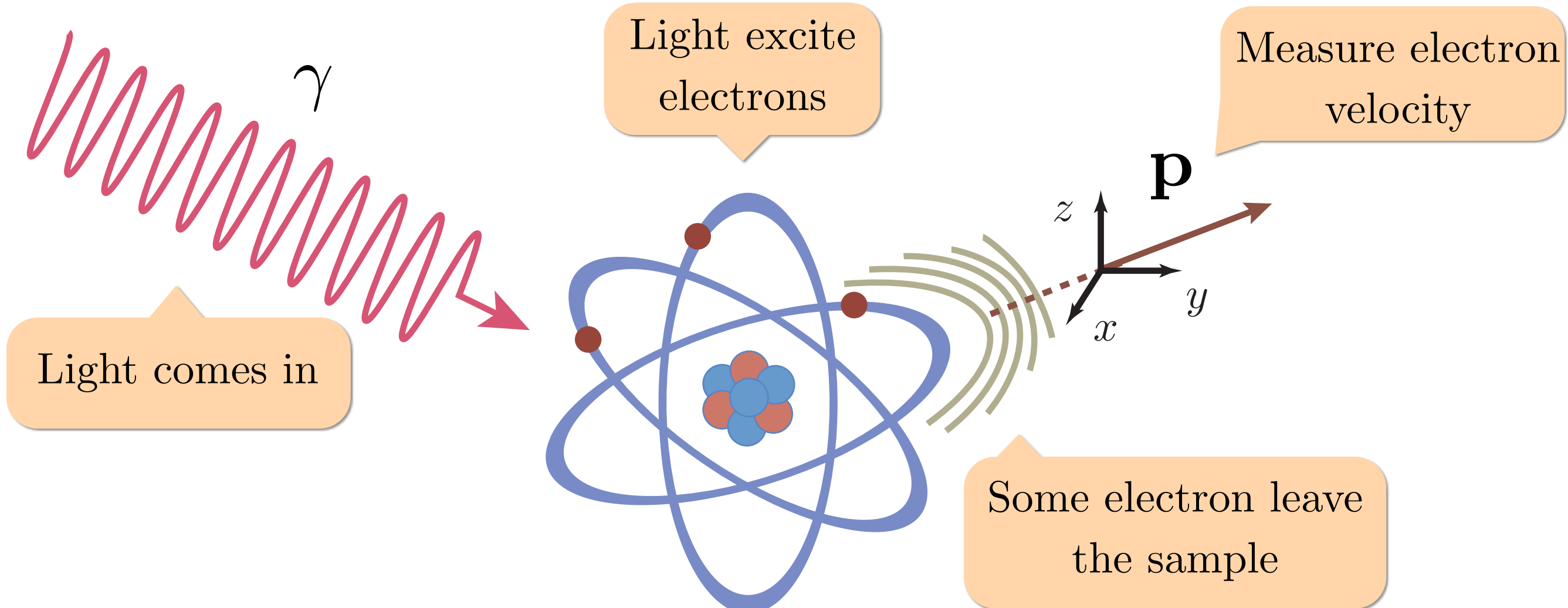
- Validation and applications:

**Hydrogen, Nitrogen dimer, Benzene, Carbon monoxide**

- Conclusions

# Photoelectron Spectroscopy

Widely used technique to analyze electronic structure of complex systems based on photoelectric effect.



Different incident light parameters allow to analyze different properties of the sample

# Photoelectron Spectroscopy

Low light intensity:

Linear regime

Electron absorbs single photon and escapes from the system

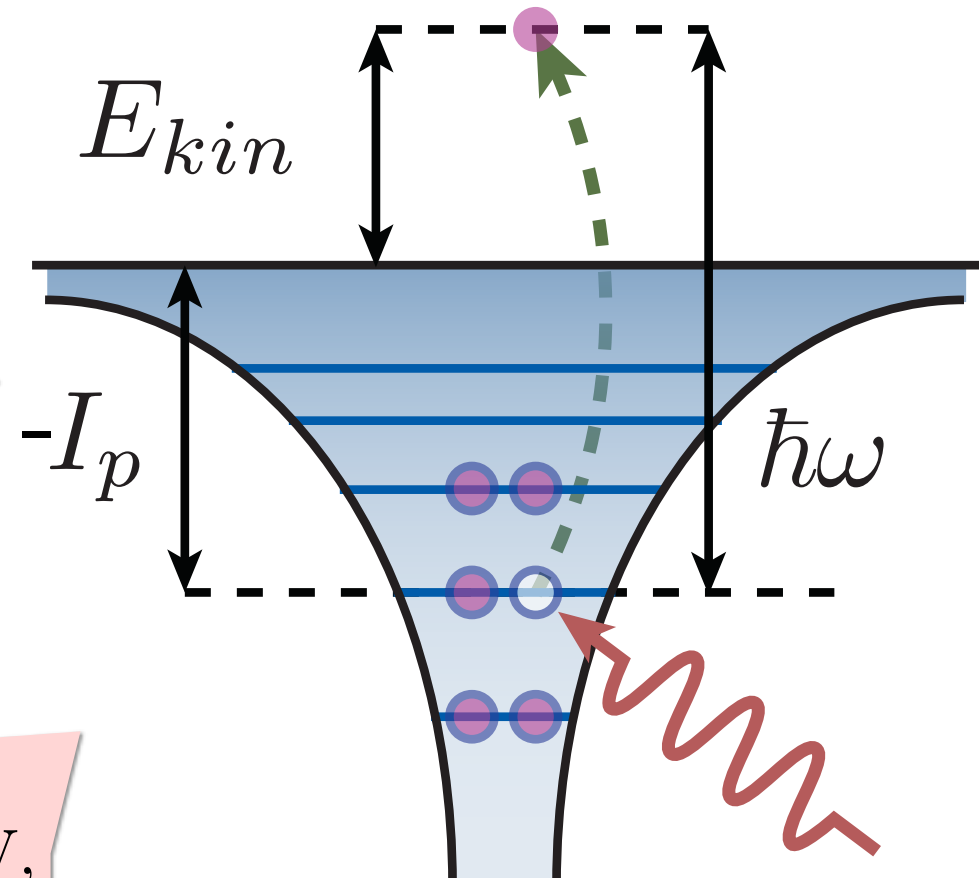
$$E_{kin} = \hbar\omega - I_p$$

OUT      IN      unknown

One step model

The larger  $\omega$  (UV, XUV, X etc.) the deeper the state probed

Angular distribution carry information on wf and molecular geometry



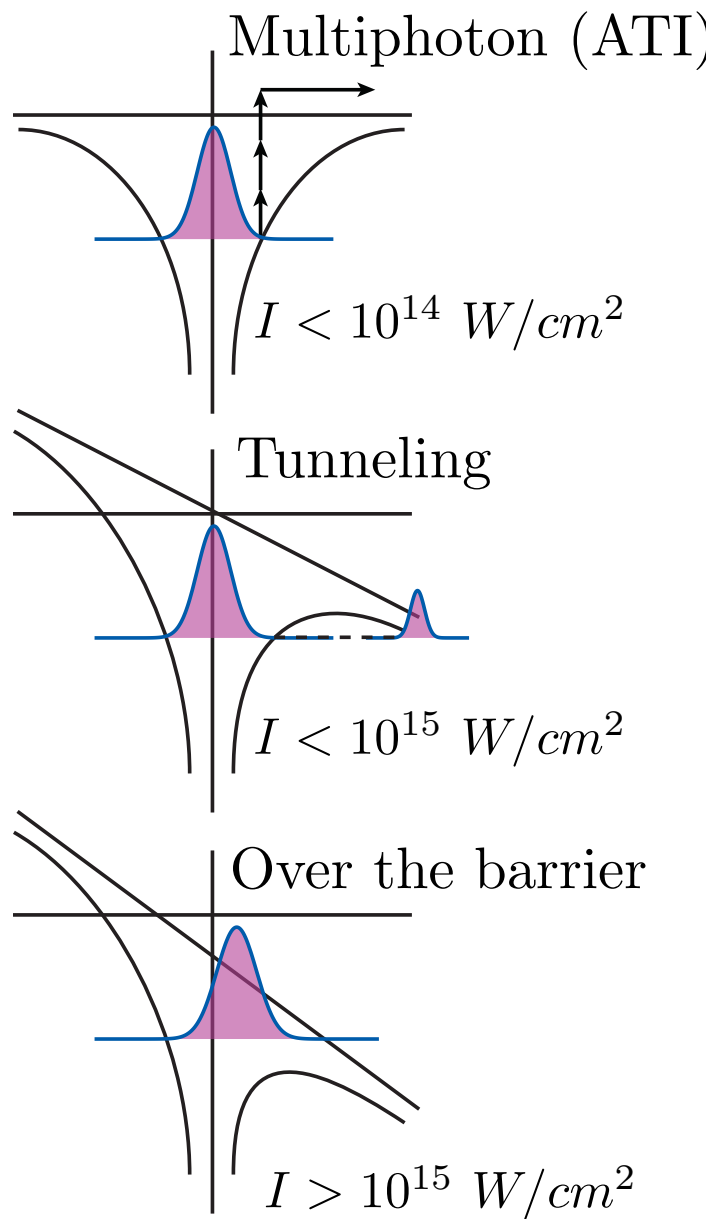
# Photoelectron Spectroscopy

Intense laser sources: Non linear phenomena

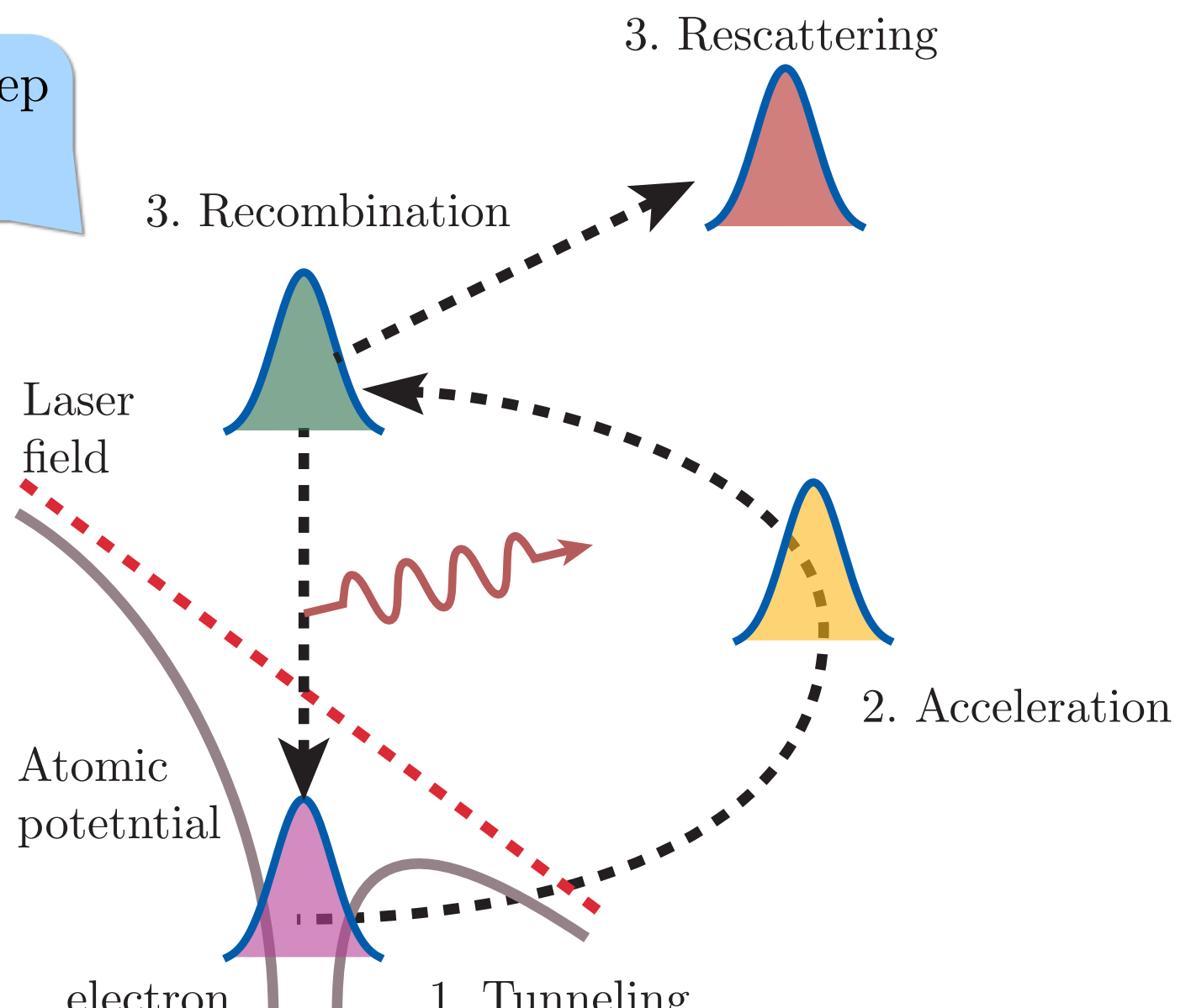
Hydrogen

$$E = \frac{e}{4\pi\epsilon_0 a_0^2} \simeq 5 \times 10^9 V cm^{-1}$$

$$I = \frac{1}{2}\epsilon_0 c E^2 \approx 3.51 \times 10^{16} W/cm^2$$

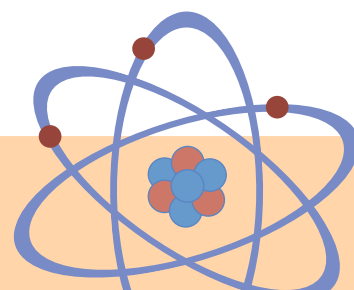


Three step model



# Modeling photoelectron spectra

Approximation hierarchy (very simplified)



Time dependent Shrödinger equation (TDSE)

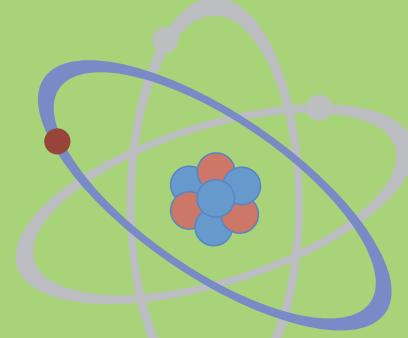
Exact many-body  
(in 3D space)

## Time Dependent Density Functional Theory (TDDFT)

Small molecules

Single active electron (SAE)

- Strong field approximation (SFA)
- Semiclassical
- Floquet

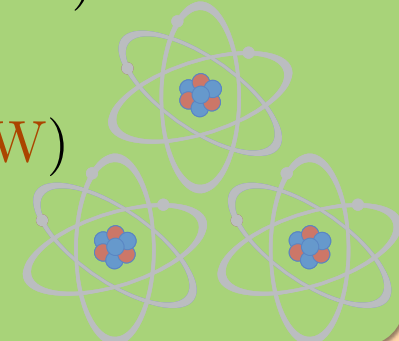


Strong laser

Fermi Golden Rule

$$\sum_i |\langle \Psi_f | H | \Psi_i \rangle|^2 \delta(E_f - E_i - \omega)$$

- Independent atomic center approximation (IAC)
- Plane wave (PW)

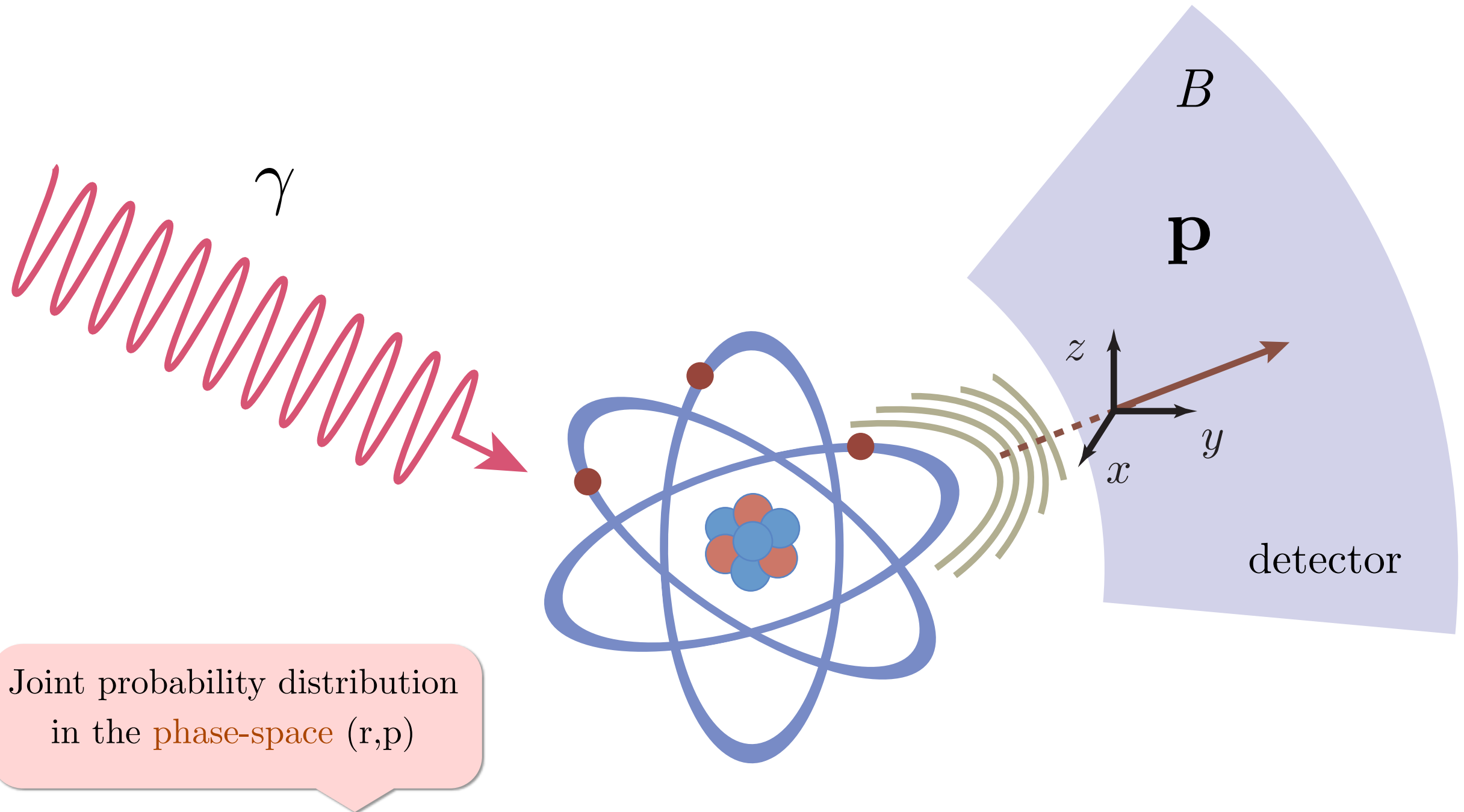


Weak laser

**What is the Phototlectron spectrum density functional?**

# Modeling photoelectron spectra

The observable is the escaping electron momentum measured at the detector.



Phase-space geometrical interpretation  
Probability to register an electron with a momentum  $p$   
in certain region of space ( $r$ )

# Modeling photoelectron spectra

Connection to the quantum realms given by the Wigner transform of one-body density matrix

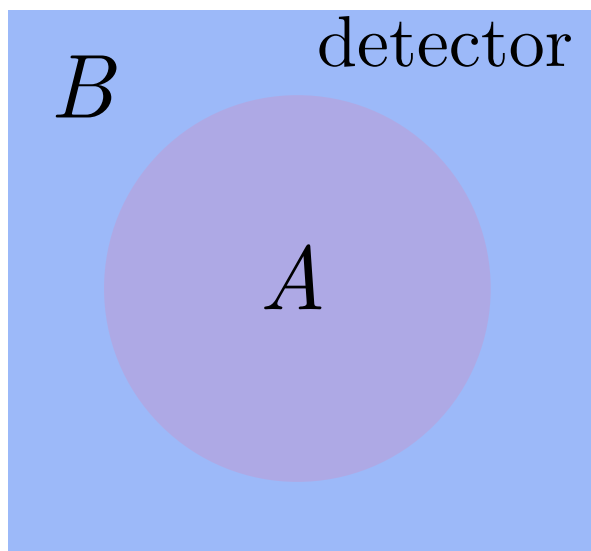
$$w(\mathbf{R}, \mathbf{p}, t) = \int \frac{d\mathbf{s}}{(2\pi)^{\frac{d}{2}}} e^{i\mathbf{p} \cdot \mathbf{s}} \rho(\mathbf{R} + \mathbf{s}/2, \mathbf{R} - \mathbf{s}/2, t)$$
$$\mathbf{R} = (\mathbf{r} + \mathbf{r}')/2$$
$$\mathbf{s} = \mathbf{r} - \mathbf{r}'$$

it is not a **joint probability** (uncertainty principle) and it can be **negative**

The Wigner function is a **quasi-probability** distribution satisfying:

$$\int d^3 R w(\mathbf{R}, \mathbf{p}) = n(\mathbf{p})$$

$$\int \frac{d^3 p}{(2\pi)^3} w(\mathbf{R}, \mathbf{p}) = n(\mathbf{R})$$



***momentum-resolved*** photoelectron spectrum

$$\mathcal{P}(\mathbf{p}) = \lim_{t \rightarrow \infty} \int_B d\mathbf{R} w(\mathbf{R}, \mathbf{p}, t)$$

# Modeling photoelectron spectra

From many body wave function to single particle theory (TDDFT).

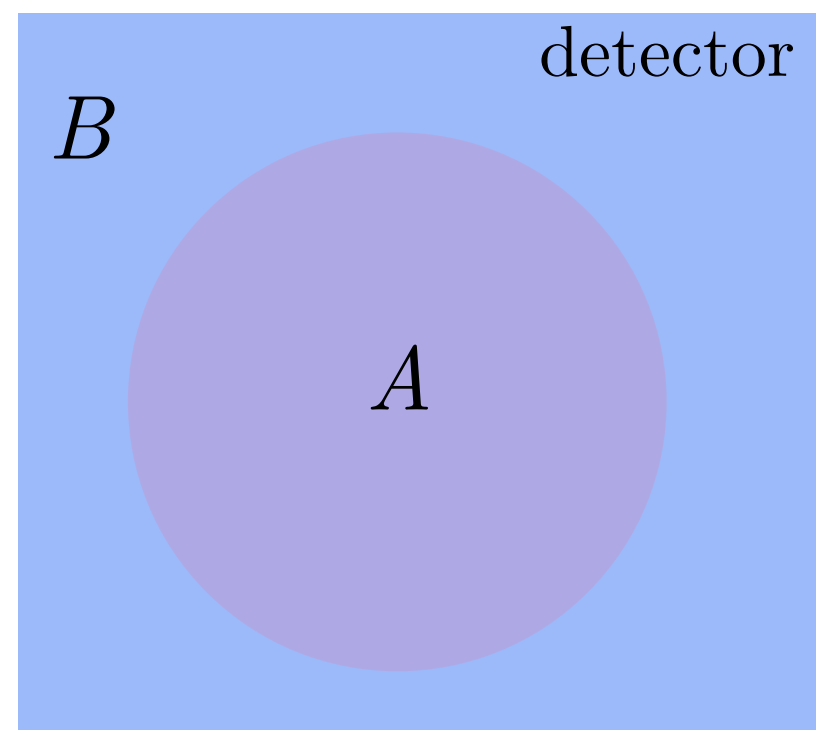
$\Psi_{KS}(\mathbf{r}_1, \dots, \mathbf{r}_N)$  single Slater determinant  $\psi_i(\mathbf{r})$

Decompose orbitals according to spatial partition

$$\psi_i(\mathbf{r}) = \varphi_{A,i}(\mathbf{r}) + \varphi_{B,i}(\mathbf{r})$$

mainly localized in  $A$

mainly localized in  $B$



$$\mathcal{P}(\mathbf{p}) \approx \sum_{i=1}^{\text{occ.}} |\tilde{\varphi}_{B,i}(\mathbf{p})|^2 \quad t \rightarrow \infty$$

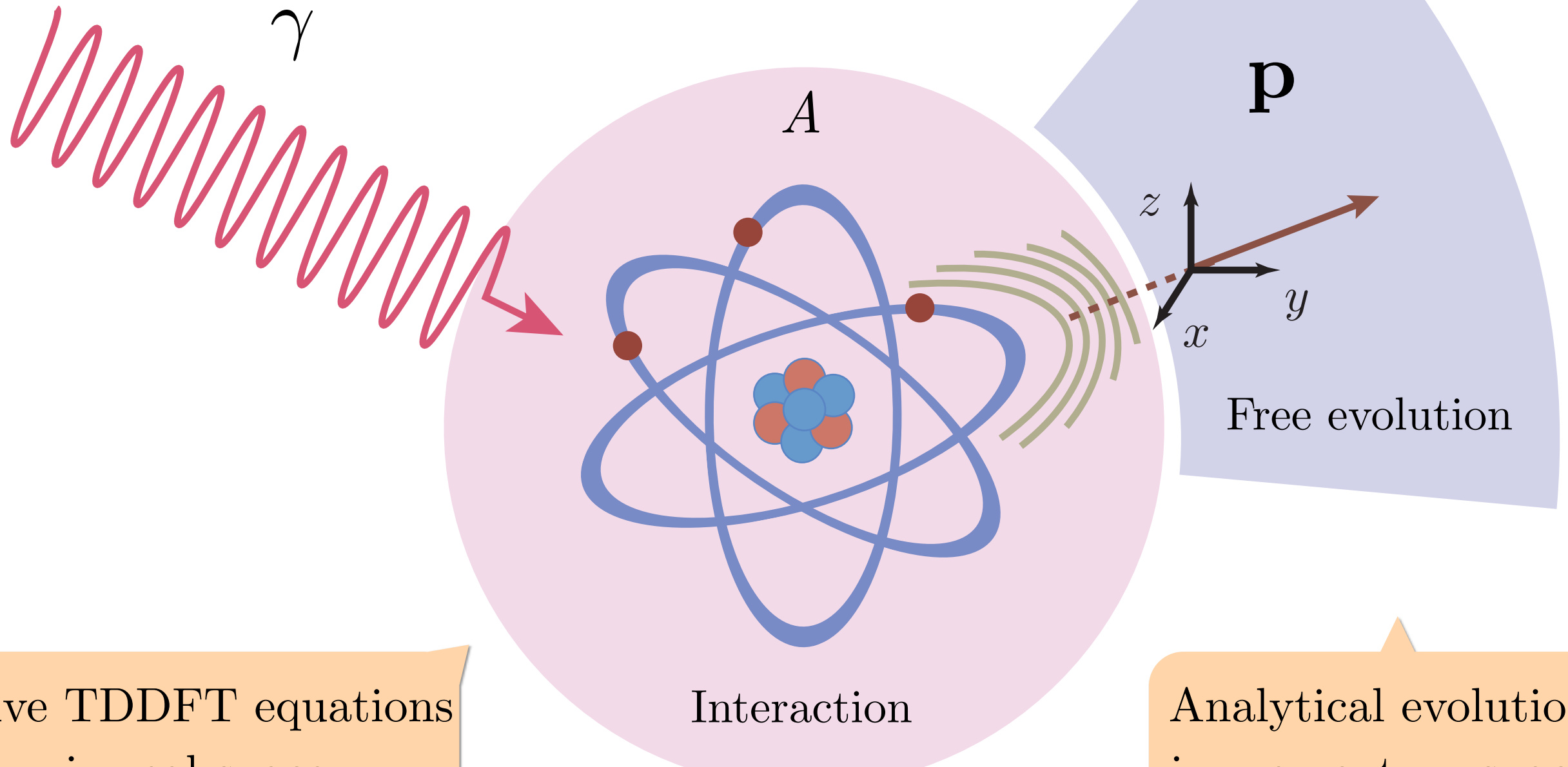
+ PES as a sum of the Fourier component of each orbital in the detector region.

+ Not only TDDFT, but also other single particle theory (HF, TDSE)

- Need large simulation boxes (typically hundreds a.u.)

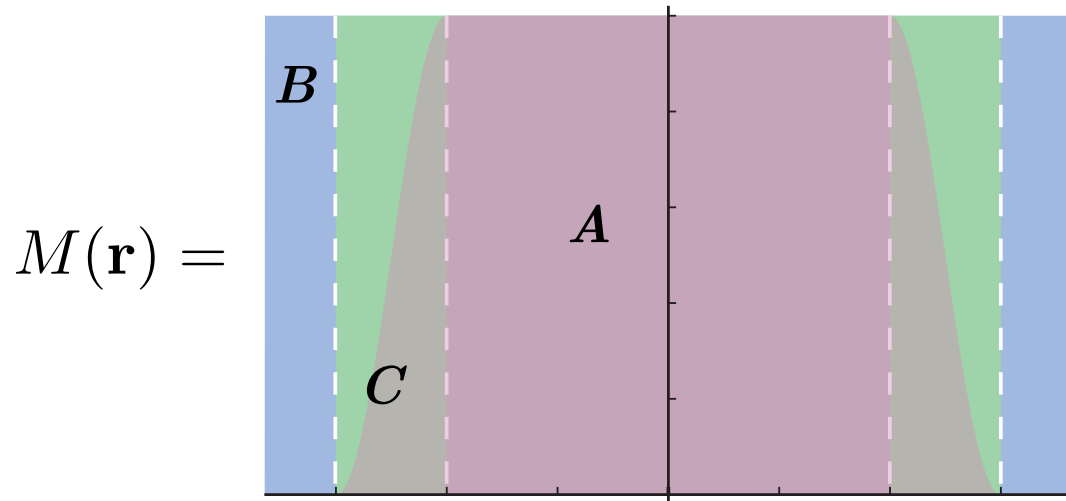
# Modeling photoelectron spectra

## Split evolution scheme



# Modeling photoelectron spectra

## Evolution scheme

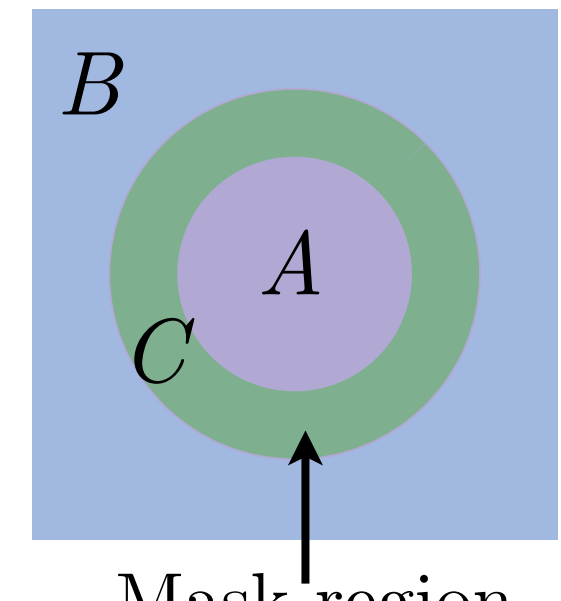


For every KS orbital

$$\varphi(\mathbf{r}, t) = M(\mathbf{r})\varphi_A(\mathbf{r}, t) + (1 - M(\mathbf{r}))\varphi_B(\mathbf{r}, t)$$

Mixed Real Fourier-space scheme

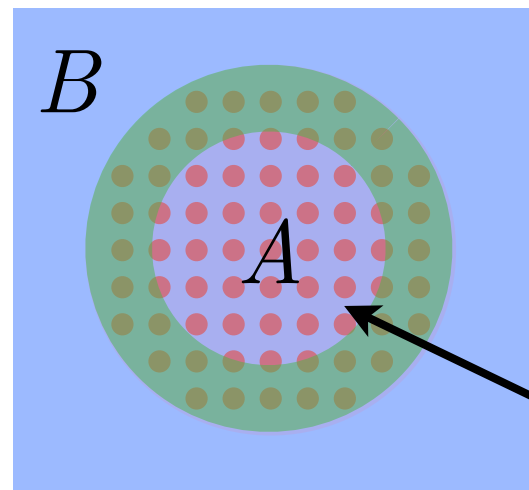
$$\begin{cases} \varphi_A(r, t') = M(r)U(t, t')(\varphi_A(r, t) + \int dp \tilde{\varphi}_B(p, t)e^{ipr}) \\ \tilde{\varphi}_B(p, t') = \int dr (1 - M(r))U(t, t')(\varphi_A(r, t) + \varphi_B(r, t))e^{-ipr} \end{cases}$$



Time propagator. If associated with **full Hamiltonian** including the external laser field the scheme is **equivalent** to integrate the evolution equations in the **whole space**

# Modeling photoelectron spectra

## The Full Mask Method (FMM)



$$\begin{cases} \varphi_{A,i}(\mathbf{r}, t') = \eta_{A,i}(\mathbf{r}, t') + \eta_{B,i}(\mathbf{r}, t') \\ \tilde{\varphi}_{B,i}(\mathbf{p}, t') = \tilde{\xi}_{A,i}(\mathbf{p}, t') + \tilde{\xi}_{B,i}(\mathbf{p}, t') \end{cases}$$

$$\eta_{A,i}(\mathbf{r}, t') = M(\mathbf{r})U(t', t)\varphi_{A,i}(\mathbf{r}, t)$$

$$\eta_{B,i}(\mathbf{r}, t') = M(\mathbf{r}) \int \frac{d\mathbf{p} e^{i\mathbf{p}\cdot\mathbf{r}}}{(2\pi)^{\frac{d}{2}}} U_V(t', t) \tilde{\varphi}_{B,i}(\mathbf{p}, t)$$

$$\tilde{\xi}_{A,i}(\mathbf{p}, t') = \int \frac{d\mathbf{r} e^{-i\mathbf{p}\cdot\mathbf{r}}}{(2\pi)^{\frac{d}{2}}} (1 - M(\mathbf{r}))U(t', t)\varphi_{A,i}(\mathbf{r}, t)$$

$$\tilde{\xi}_{B,i}(\mathbf{p}, t') = U_V(t', t)\tilde{\varphi}_{B,i}(\mathbf{p}, t) - \int \frac{d\mathbf{r} e^{-i\mathbf{p}\cdot\mathbf{r}}}{(2\pi)^{\frac{d}{2}}} \eta_{B,i}(\mathbf{r}, t')$$

Can evaluate with  
discrete FT

localized in momentum  
localized in space  
(buffer region)

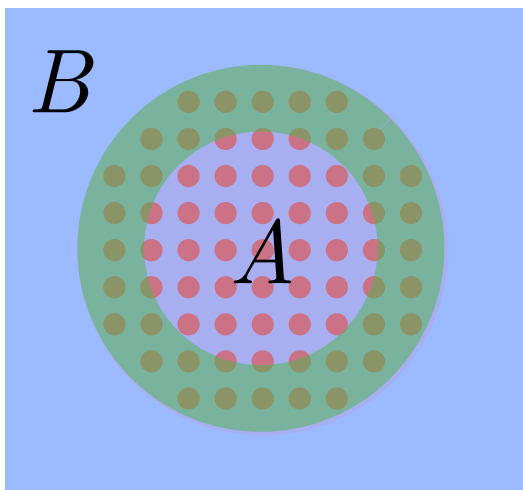
TDDFT propagator  
 $U(t, t')$

Volkov propagator (free  $\mathbf{e}$  in td field)  

$$U_V(t', t) = \exp \left\{ -i \int_t^{t'} d\tau \frac{1}{2} \left[ \mathbf{p} - \frac{\mathbf{A}(\tau)}{c} \right]^2 \right\}$$

# Modeling photoelectron spectra

## The Mask Method (MM)



If region A is big enough electron flow from B to A is negligible

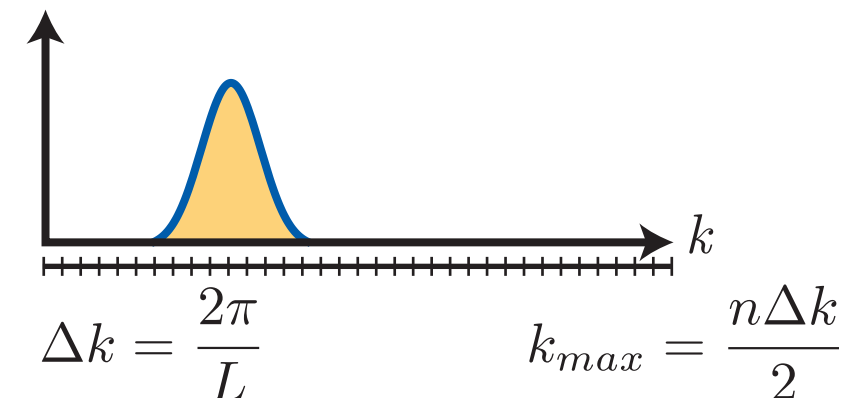
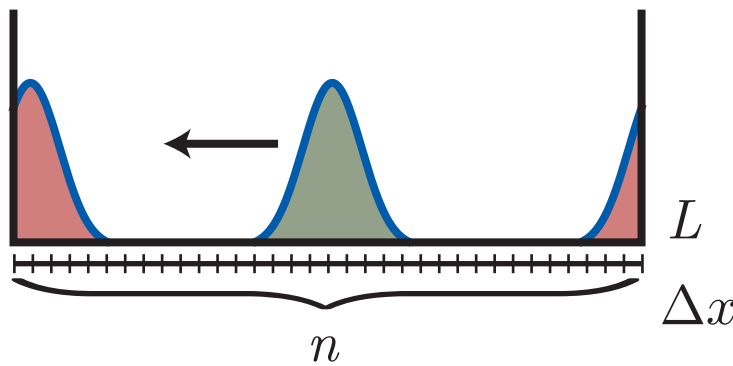
$$\begin{cases} \varphi_{A,i}(\mathbf{r}, t') = \eta_{A,i}(\mathbf{r}, t') + \cancel{\eta_{B,i}(\mathbf{r}, t')} \\ \tilde{\varphi}_{B,i}(\mathbf{p}, t') = \tilde{\xi}_{A,i}(\mathbf{p}, t') + \tilde{\xi}_{B,i}(\mathbf{p}, t') \end{cases}$$

$$\begin{aligned} \eta_{A,i}(\mathbf{r}, t') &= M(\mathbf{r})U(t', t)\varphi_{A,i}(\mathbf{r}, t) \\ \cancel{\eta_{B,i}(\mathbf{r}, t')} &= M(\mathbf{r}) \int \frac{d\mathbf{p} e^{i\mathbf{p}\cdot\mathbf{r}}}{(2\pi)^{\frac{d}{2}}} U_V(t', t) \tilde{\varphi}_{B,i}(\mathbf{p}, t) \\ \tilde{\xi}_{A,i}(\mathbf{p}, t') &= \int \frac{d\mathbf{r} e^{-i\mathbf{p}\cdot\mathbf{r}}}{(2\pi)^{\frac{d}{2}}} (1 - M(\mathbf{r}))U(t', t)\varphi_{A,i}(\mathbf{r}, t) \\ \tilde{\xi}_{B,i}(\mathbf{p}, t') &= U_V(t', t)\tilde{\varphi}_{B,i}(\mathbf{p}, t) - \int \frac{d\mathbf{r} e^{-i\mathbf{p}\cdot\mathbf{r}}}{(2\pi)^{\frac{d}{2}}} \eta_{B,i}(\mathbf{r}, t'). \end{aligned}$$

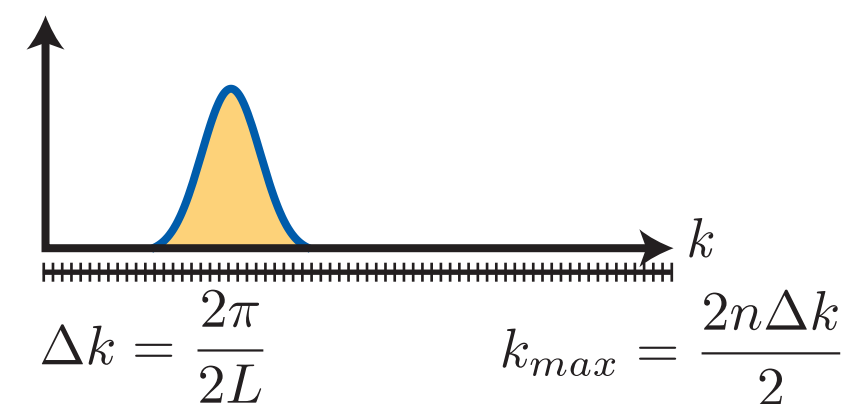
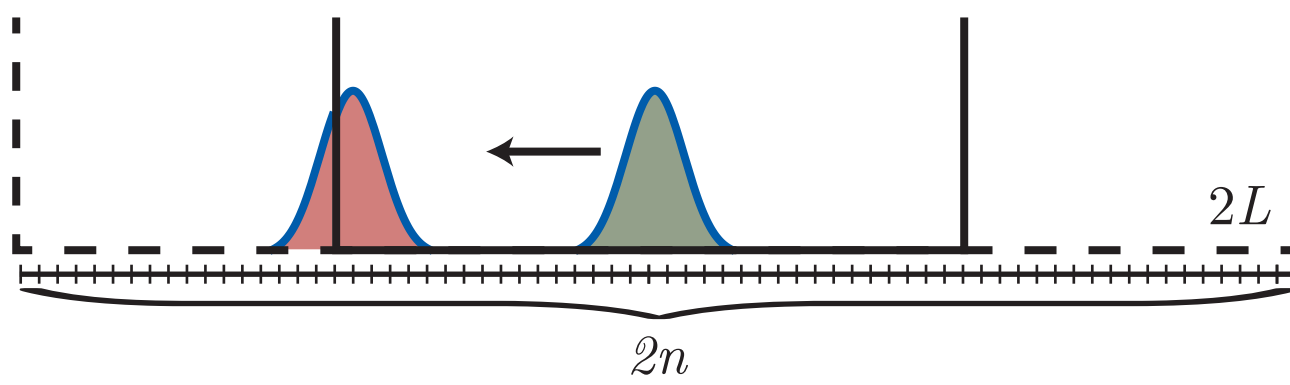
# Modeling photoelectron spectra

## The Full Mask Method (FMM): numerical stability

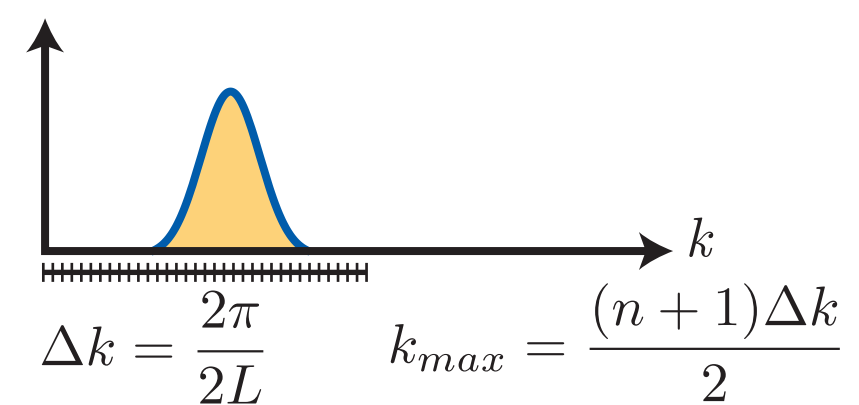
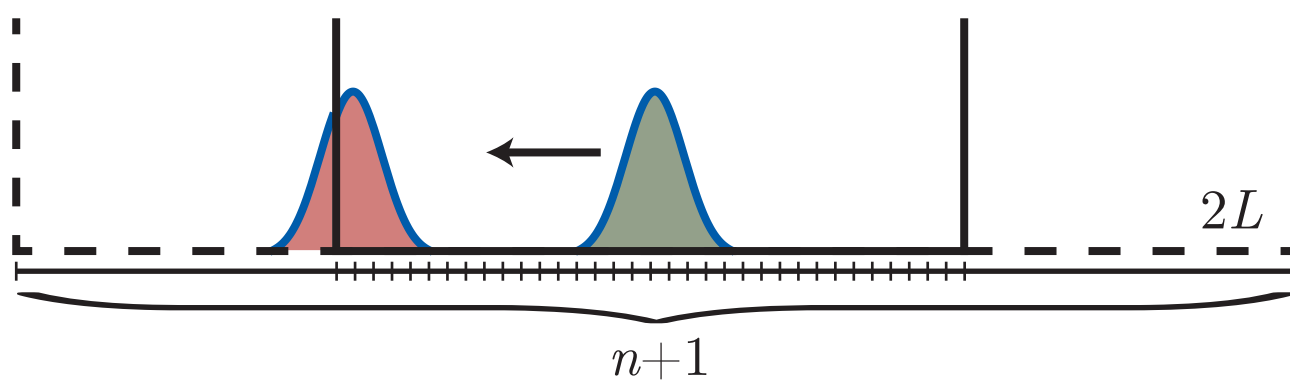
FFT



FFT - Zero padding



NFFT - Zero padding



# Modeling photoelectron spectra

Octopus inp sample



```
PhotoelectronSpectrum = pes_mask
```

mask\_mode  
passive\_mode

```
%PESMaskSize  
    5 | Radius  
%
```

```
PESMaskMode = fullmask_mode  
PESMaskPlaneWaveProjection = fft_map  
PESMaskEnlargeLev = 1  
PESMaskNFFTEnlargeLev = 0
```

nfft\_map  
pfft\_map

More info:

```
oct-help -s PESMask
```

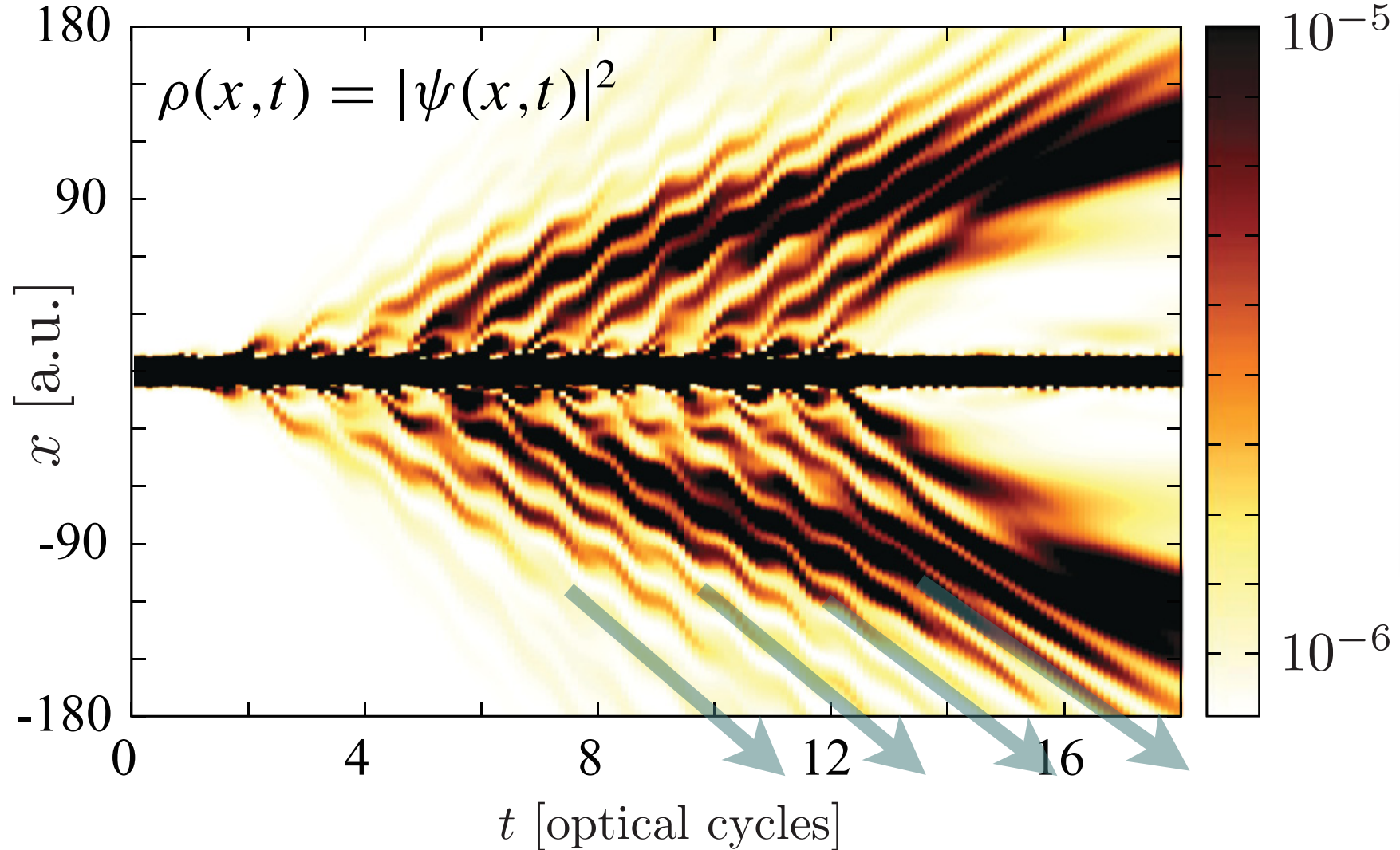
Output in `td.general/PESM*`

Post-process data:

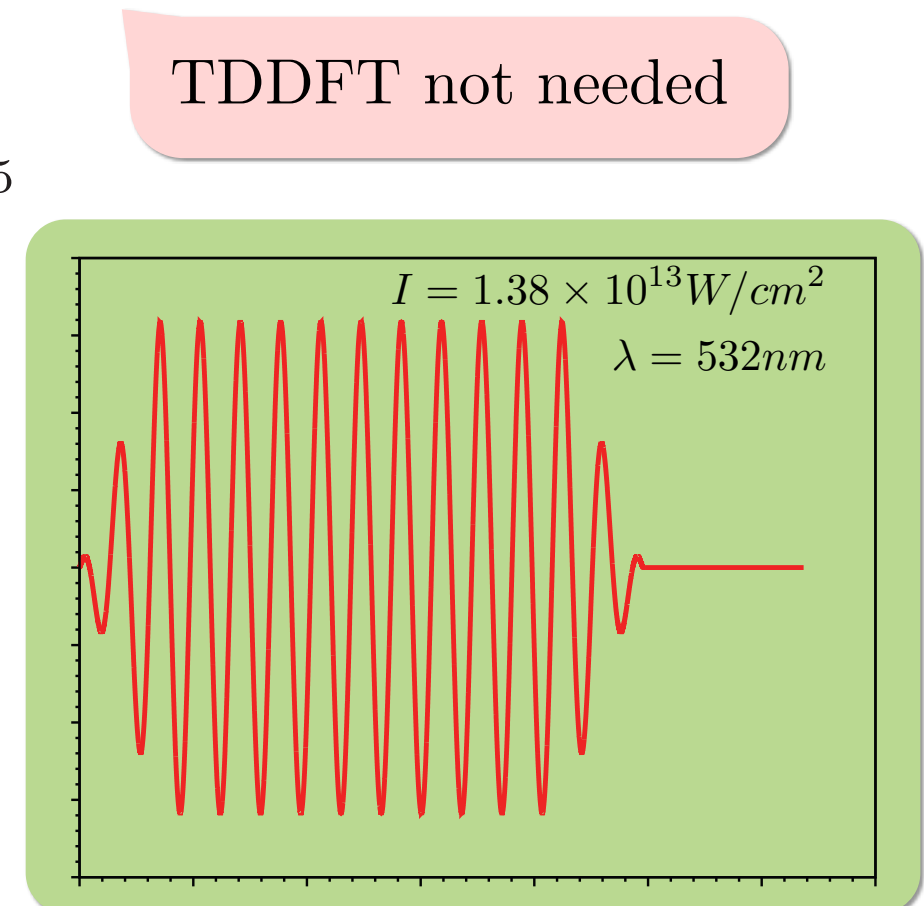
```
oct-photoelectron_spectrum --help
```

# Validation of the methods

## Multiphoton ionization of 1D soft-core hydrogen atom



Slope proportional to  
electron kinetic energy

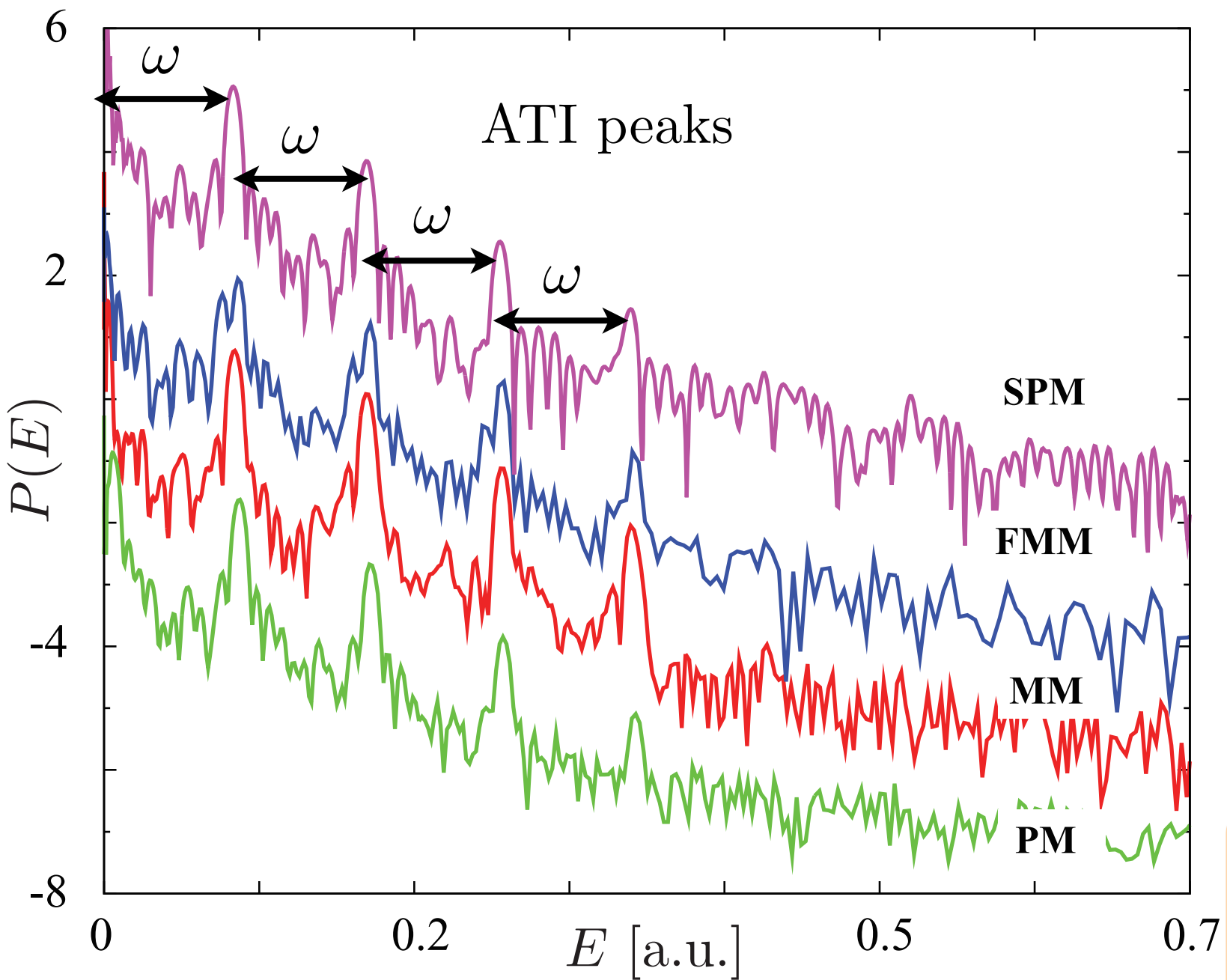


Electron-ion with  
soft Coulomb

$$V(x) = \frac{-1}{\sqrt{2 + x^2}}$$

# Validation of the methods

## Comparison of different methods for PES



$$E = s\omega - I_p - U_p$$

$$I_p = 0.5 \text{ a.u.} \quad s_{min} = 6$$

$$U_p = A_0^2/4c^2 = 0.0133 \text{ a.u.} \quad \omega = 0.0856 \text{ a.u.}$$

### Reference Methods

Passive Method (PM)

$$\mathcal{P}(\mathbf{p}) \approx \sum_{i=1}^{\text{occ.}} |\tilde{\varphi}_{B,i}(\mathbf{p})|^2$$

### Sampling Point Method (SPM)

$$P_{\mathbf{r}_S}(E) = \sum_{i=1}^{\text{occ}} |\psi_i(\mathbf{r}_S, E)|^2.$$

A. Pohl, P.-G. Reinhard, and E. Suraud,  
Phys. Rev. Lett. 84, 5090 (2000).

### Requirements

PM:  $box = 500 \text{ a.u.}$   $R_a = 30 \text{ a.u.}$

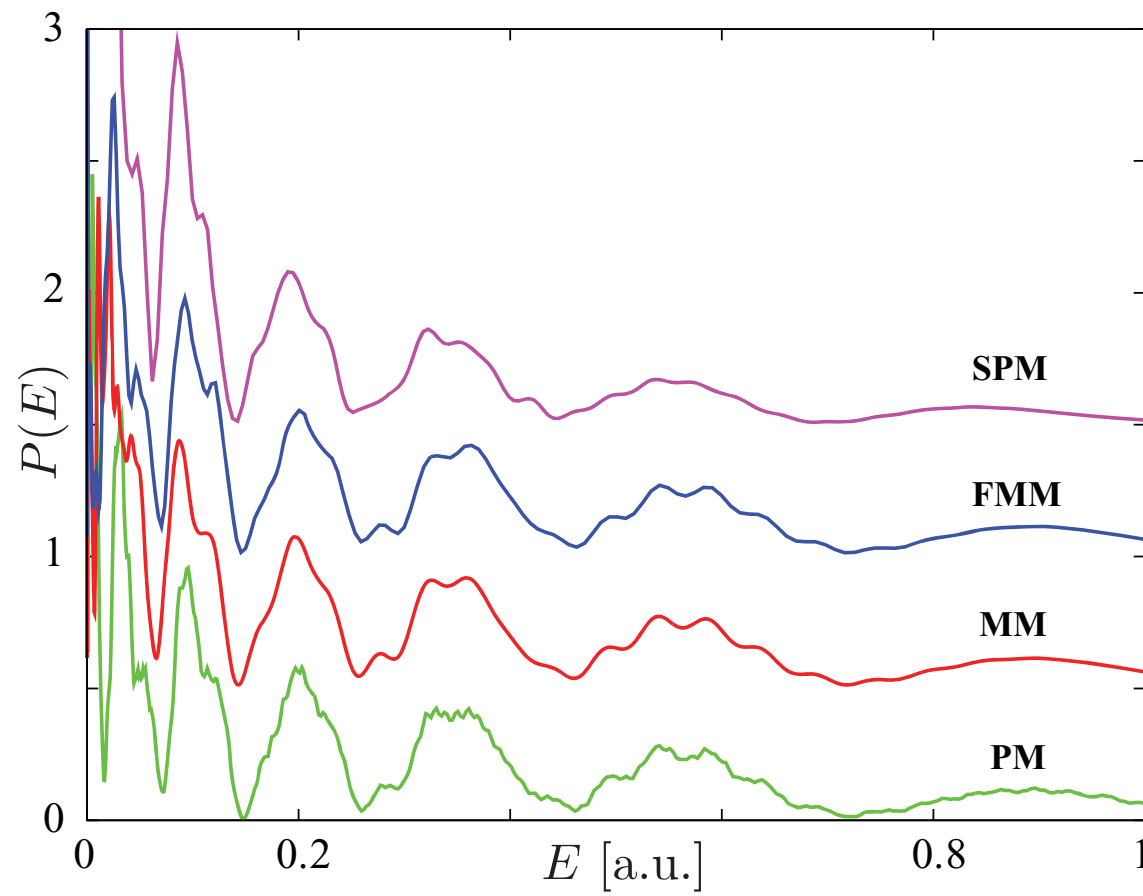
SPM:  $box = 550 \text{ a.u.}$ ,  $r_s = \pm 500 \text{ a.u.}$   
 $T = 74$  opt. cycle

FMM:  $R_a = 40 \text{ a.u.}$   $R_c = 30 \text{ a.u.}$

MM:  $R_a = 70 \text{ a.u.}$   $R_c = 30 \text{ a.u.}$

# Validation of the methods

## Ultrashort intense infrared laser



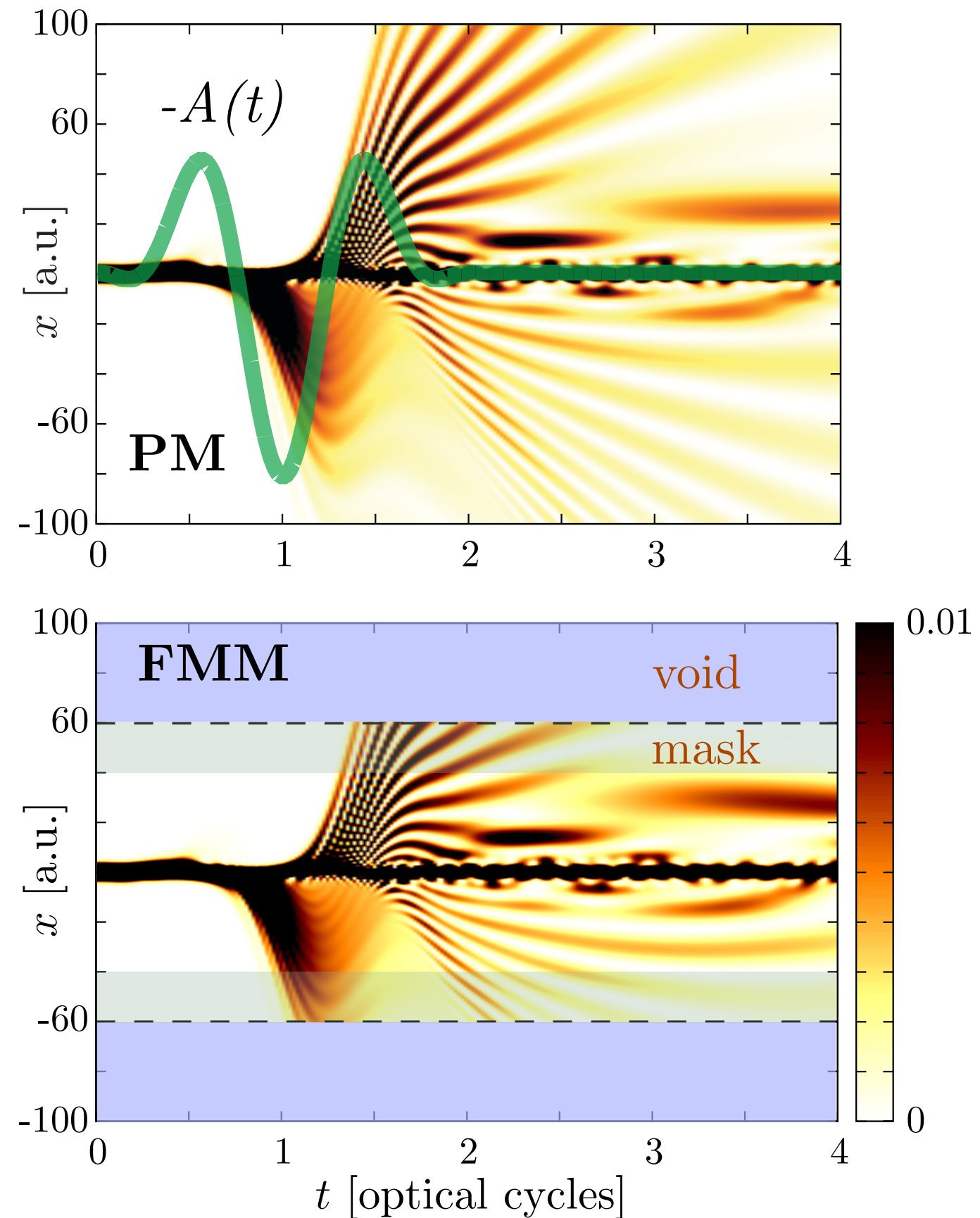
### Requirements

PM:  $box = 700a.u.$ ,  $R_a = 50a.u$

SPM:  $box = 200a.u.$ ,  $r_s = \pm 130a.u.$   
T=7 opt. cycle

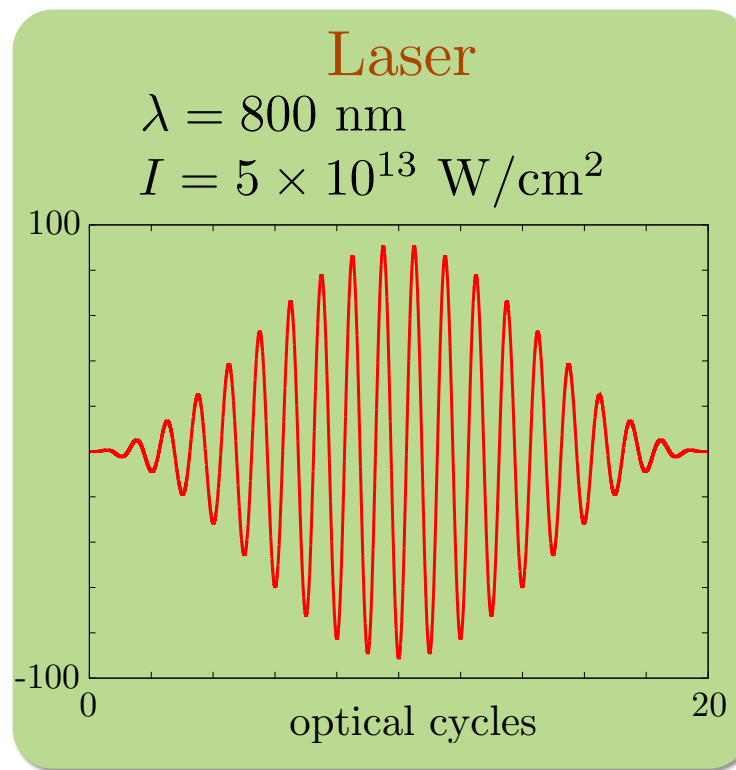
FMM:  $R_a = 60a.u.$ ,  $R_c = 40a.u.$

MM:  $R_a = 200a.u.$ ,  $R_c = 40a.u.$



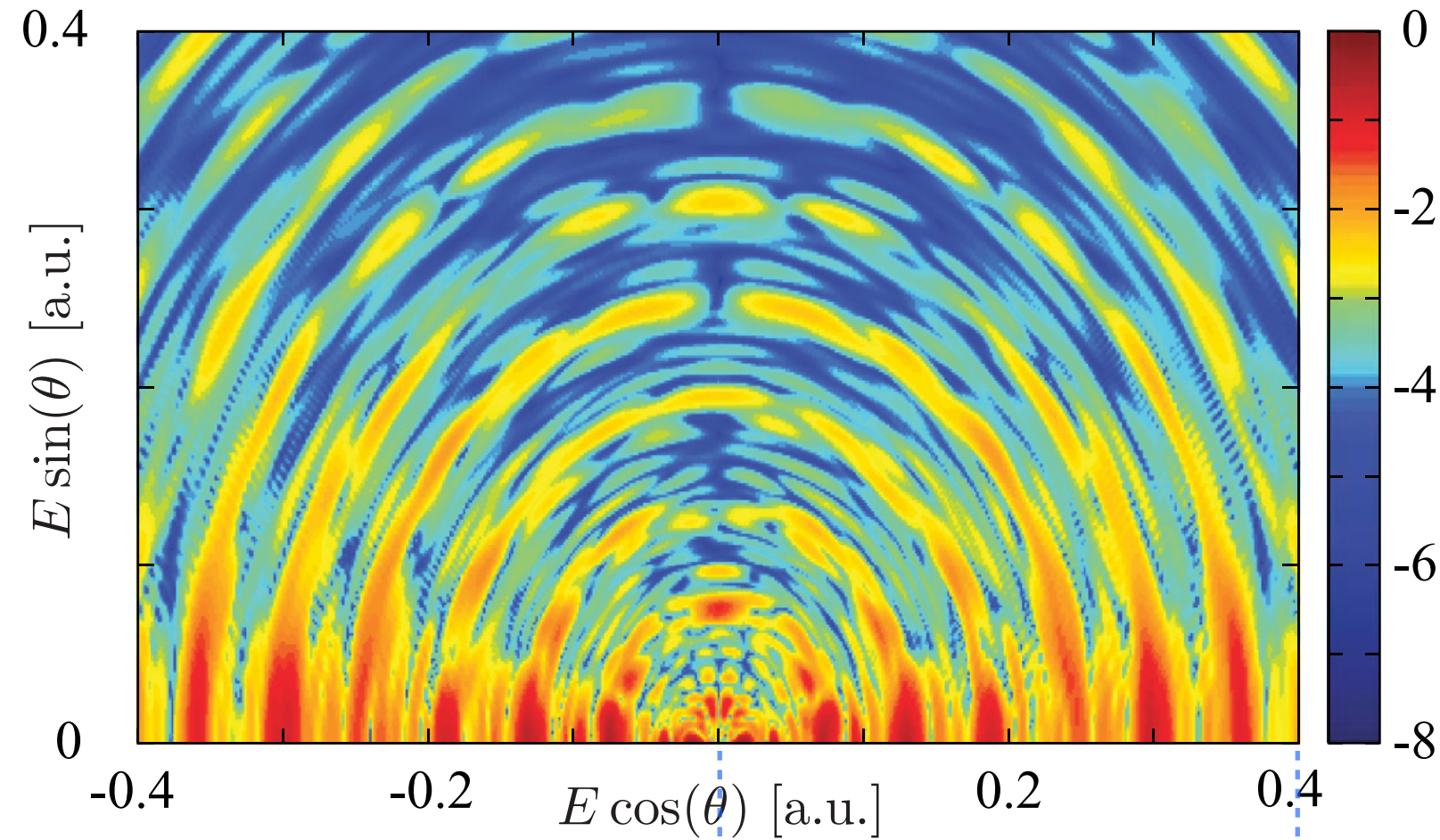
# A 3D example

Multiphoton ionization of 3D hydrogen atom: long infrared laser pulse



Requirements

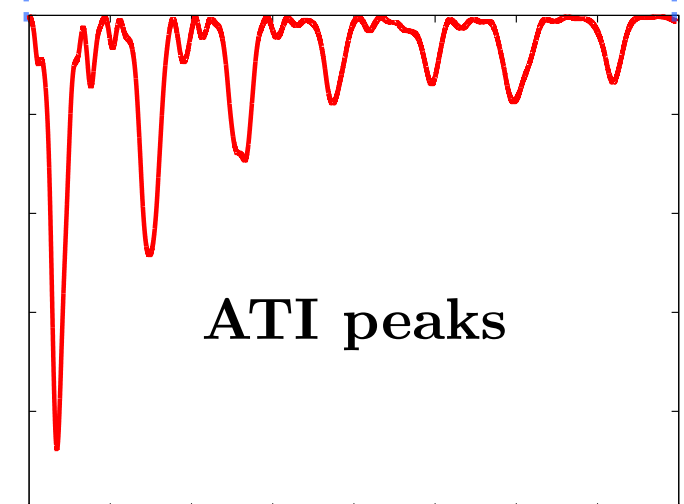
MM:  $R_A = 60 \text{ a.u.}$   $R_C = 50 \text{ a.u.}$



Rings with fine structure

1st ATI peak: nodal pattern induced by the long-range Coulomb potential.

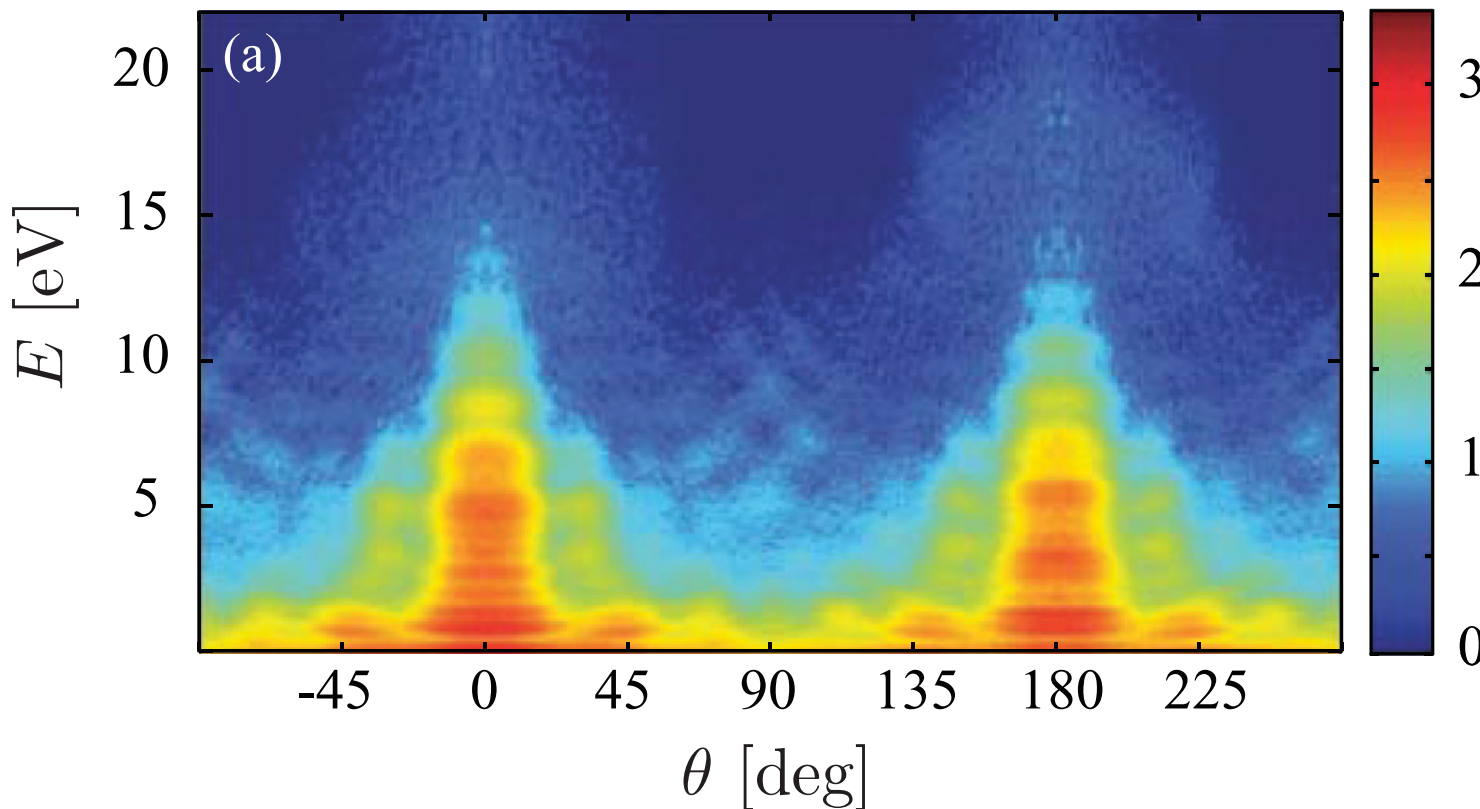
ATI peak is determined by one dominant partial wave in the final state with a given angular momentum quantum number.



Z. Zhou and S.-I. Chu, Phys. Rev. A 83, 013405 (2011)

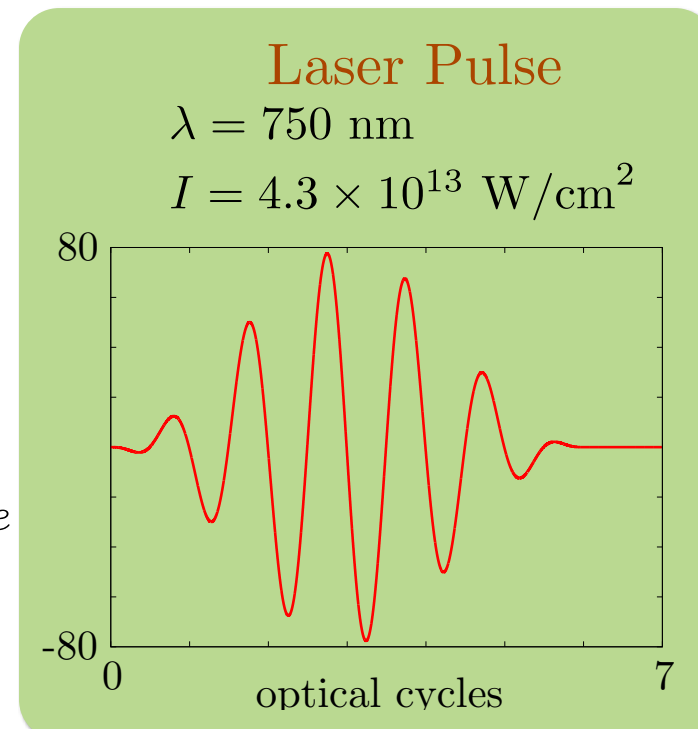
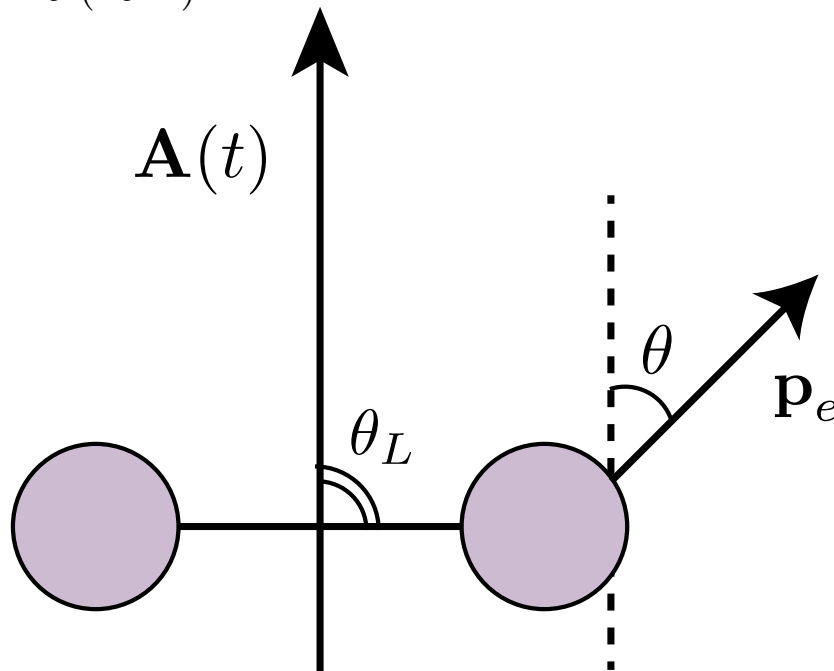
# N<sub>2</sub> under a few-cycle infrared laser pulse

Random oriented N<sub>2</sub> molecules



A. Gazibegovic-Busuladzic, et al. Phys. Rev. A 84, 043426 (2011).

TDDFT  
XC-functional: LB94 (correct asymptotic)  
Electron-ion: Trouiller-Martins pseudo  
Fixed ions  
FMM:  $R_a = 35a.u.$   $R_c = 25a.u.$

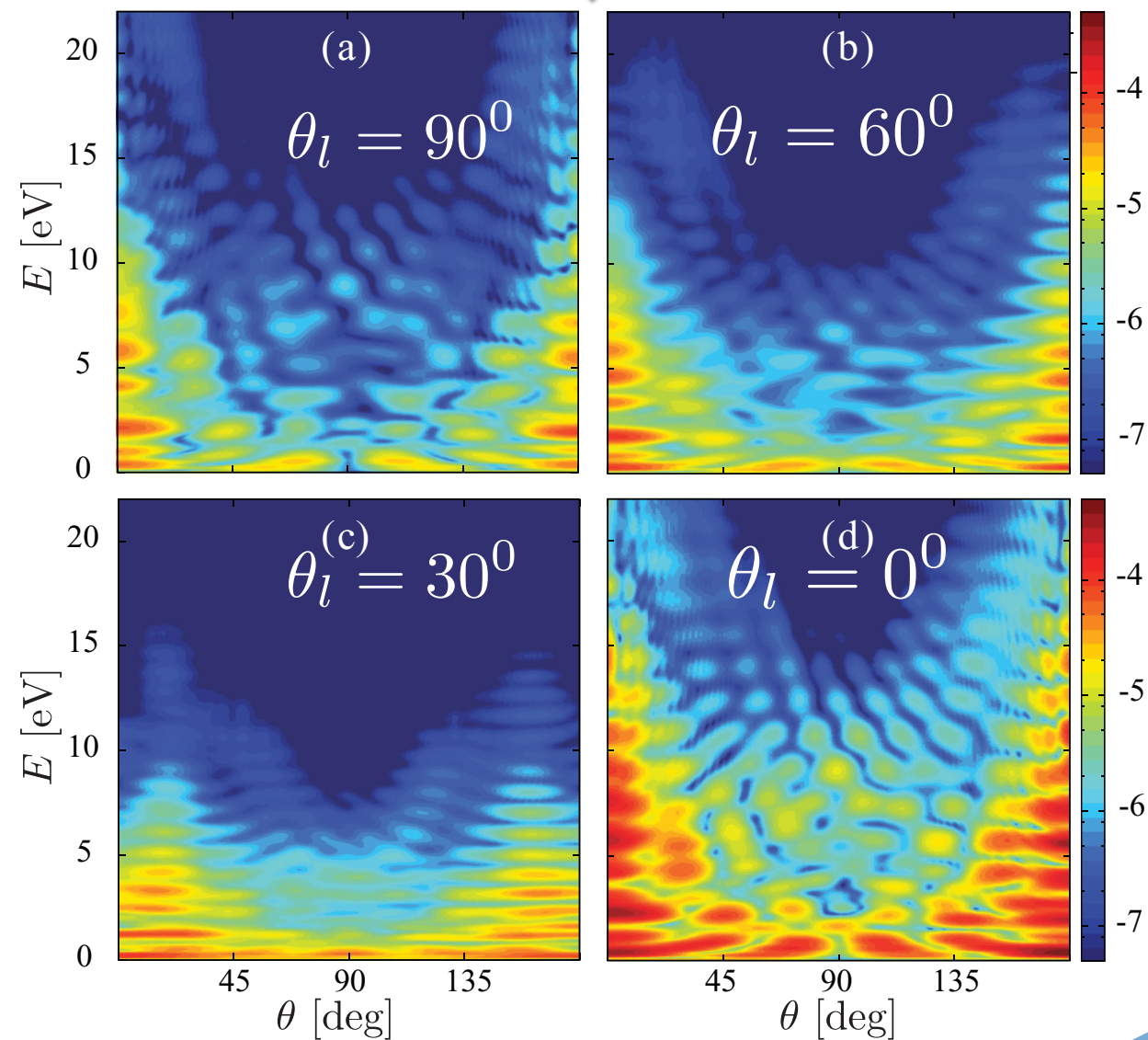


Calculations for different angle between laser polarization and molecular axis

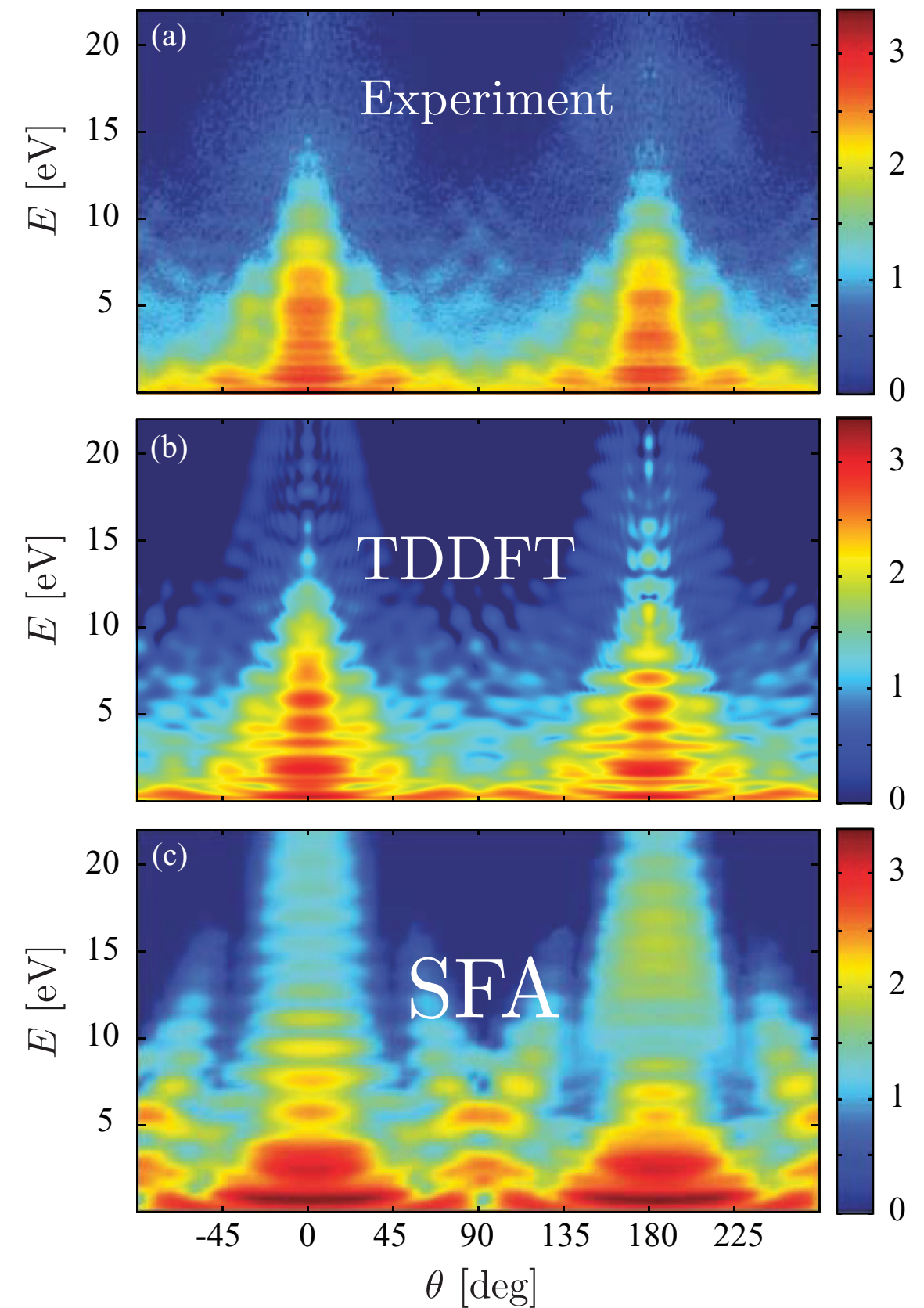
# N<sub>2</sub> under a few-cycle infrared laser pulse

Combine PAD at different relative angles

$$\bar{P}(E, \theta) \propto \int_0^{90^\circ} d\theta_L \sin \theta_L P_{\theta_L}(E, \theta).$$



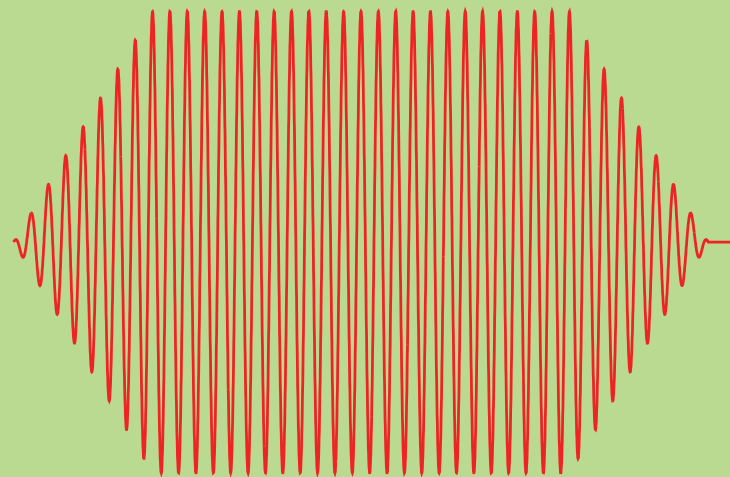
Good agreement with experiment  
Slightly deteriorates for low energies  
due to Coulomb tail not fully  
accounted for size simulation box.



A. Gazibegovic-Busuladzic, et al. Phys. Rev. A 84, 043426

## He-(I) PADs - Linear regime

$$I = 1 \times 10^8 \text{ W/cm}^2$$
$$\omega = 0.78 \text{ a.u. (UV)}$$



Weak laser, **non-linear** effects can be **neglected**  
**Fermi-Golden rule:**

$$P(\mathbf{p}) \propto \sum_i |\langle \Psi_f | \mathbf{A}_0 \cdot \mathbf{p} | \Psi_i \rangle|^2 \delta(E_f - E_i - \omega),$$

single coherent process from a molecular orbital to  
the final state, **one-step** model of photoemission

Plane Wave PW approximation:

$$\sqrt{P(\mathbf{p})} \propto \sum_i |\mathbf{A}_0 \cdot \mathbf{p}| |\tilde{\Psi}_i(\mathbf{p})|.$$

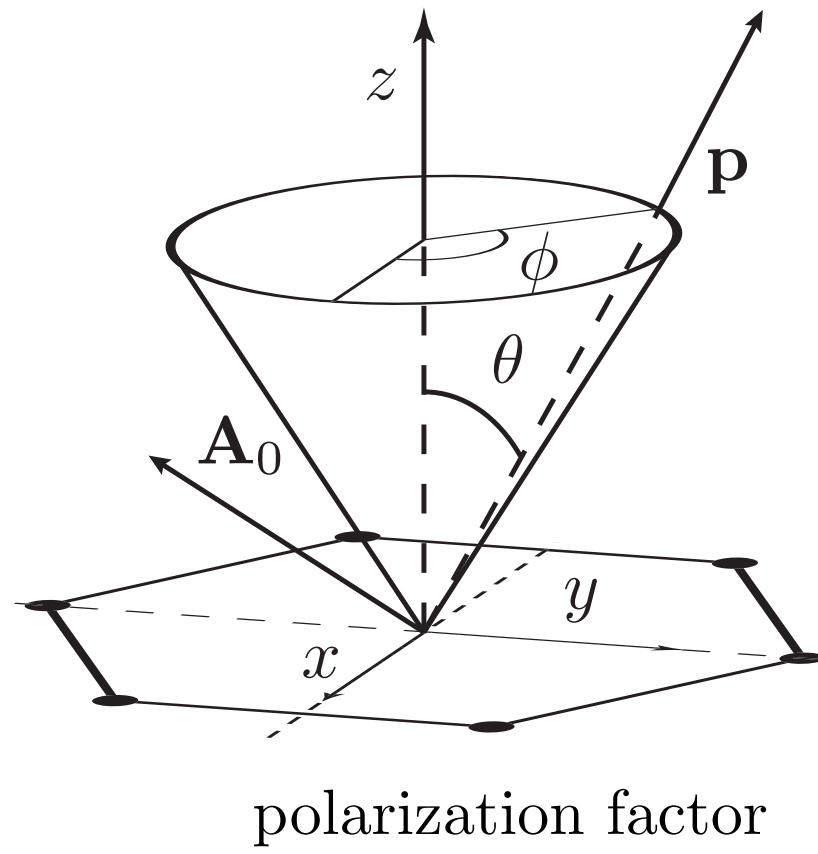
Postulated to be a good approximation for:

- (1)  **$\pi$ -conjugated planar molecules** (initial molecular orbital sum of orbital with same character)
- (2) constituted by **light atoms** (H, C, N, O)
- (3) photoelectrons emerging with **momentum** p almost parallel to the **polarization** axis.

*P. Puschnig et al. Science 326, 702 (2009).*

Discards multi-center emission effects

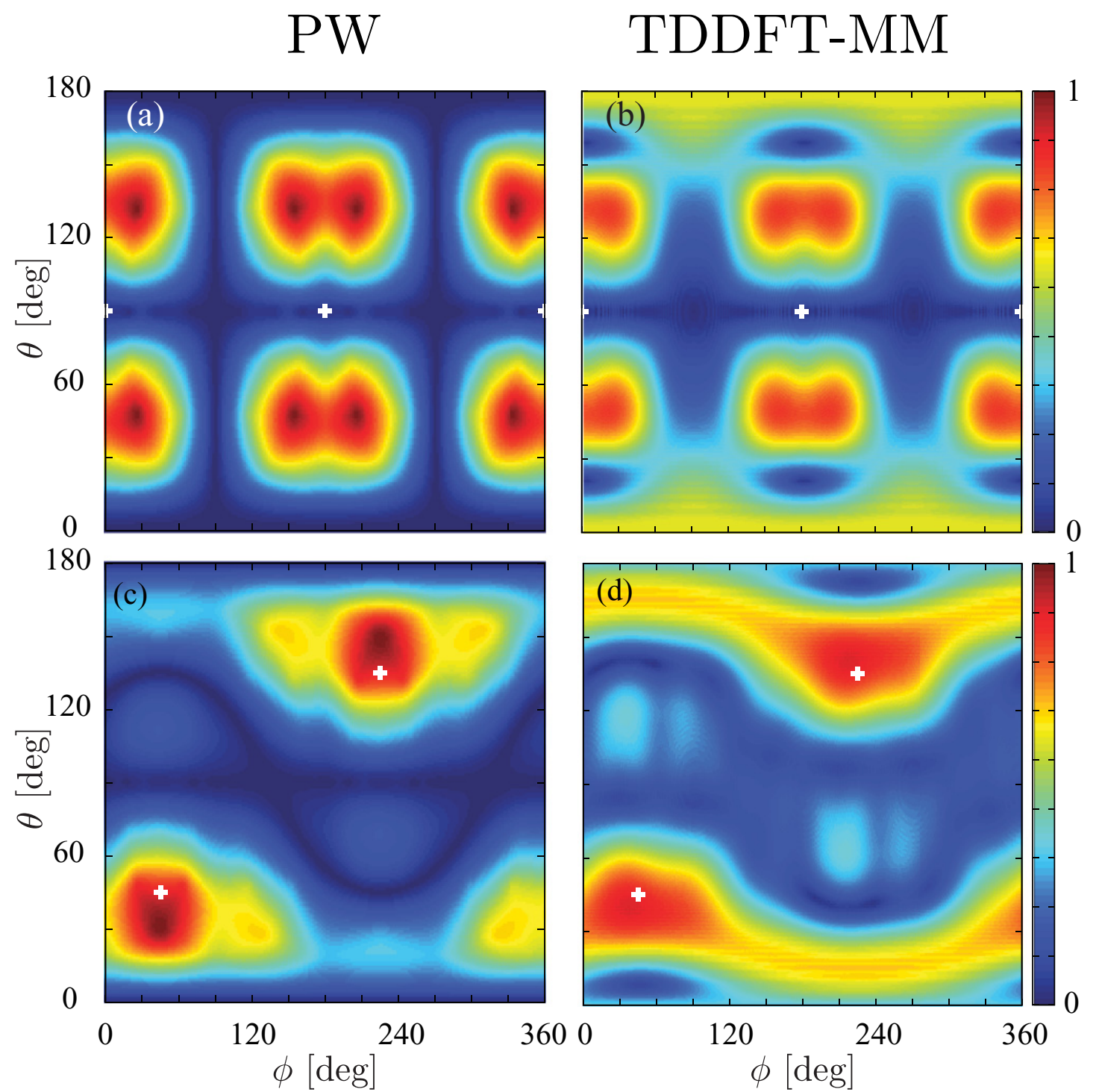
# He-(I) PADs: Benzene



$$\sqrt{P_H(\mathbf{p})} \propto |\mathbf{A}_0 \cdot \mathbf{p}| |\tilde{\Psi}_H(\mathbf{p})|,$$

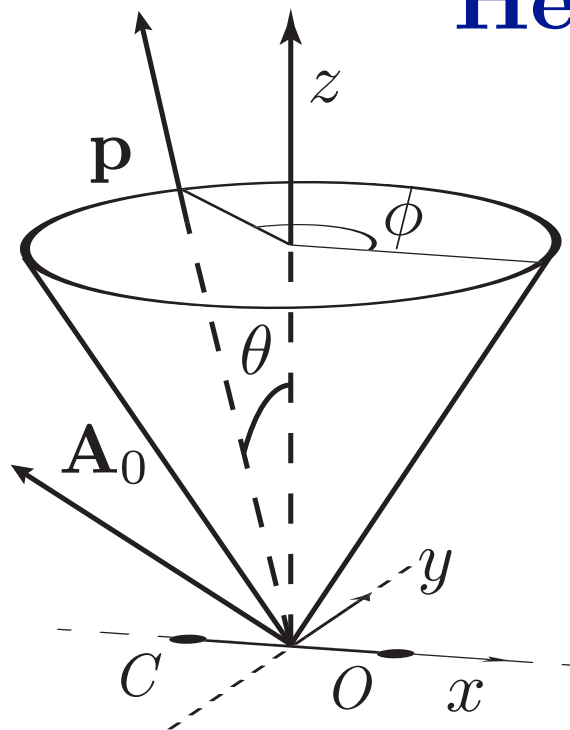
## Remarks

- PAD reminiscent of  $\pi$  symmetry
- Off-plane polarization, partially washed out due to  $\sigma$  components
- Nodes at  $\theta = 90^\circ$  due to HOMO in xy plane
- Other nodes determined by polarization factor



Reasonable overall agreement.  
Quantitative agreement close  
to polarization axis

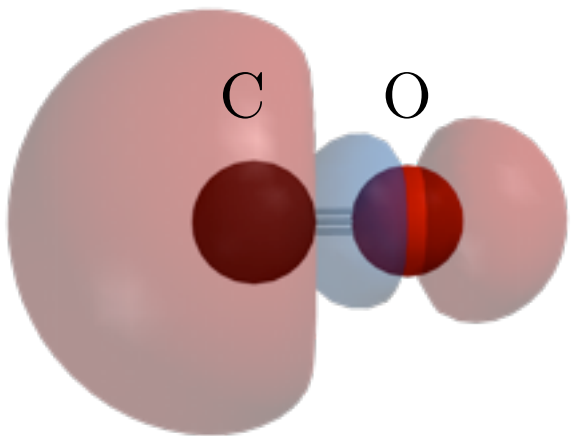
# He-(I) PADs: Carbon Monoxide



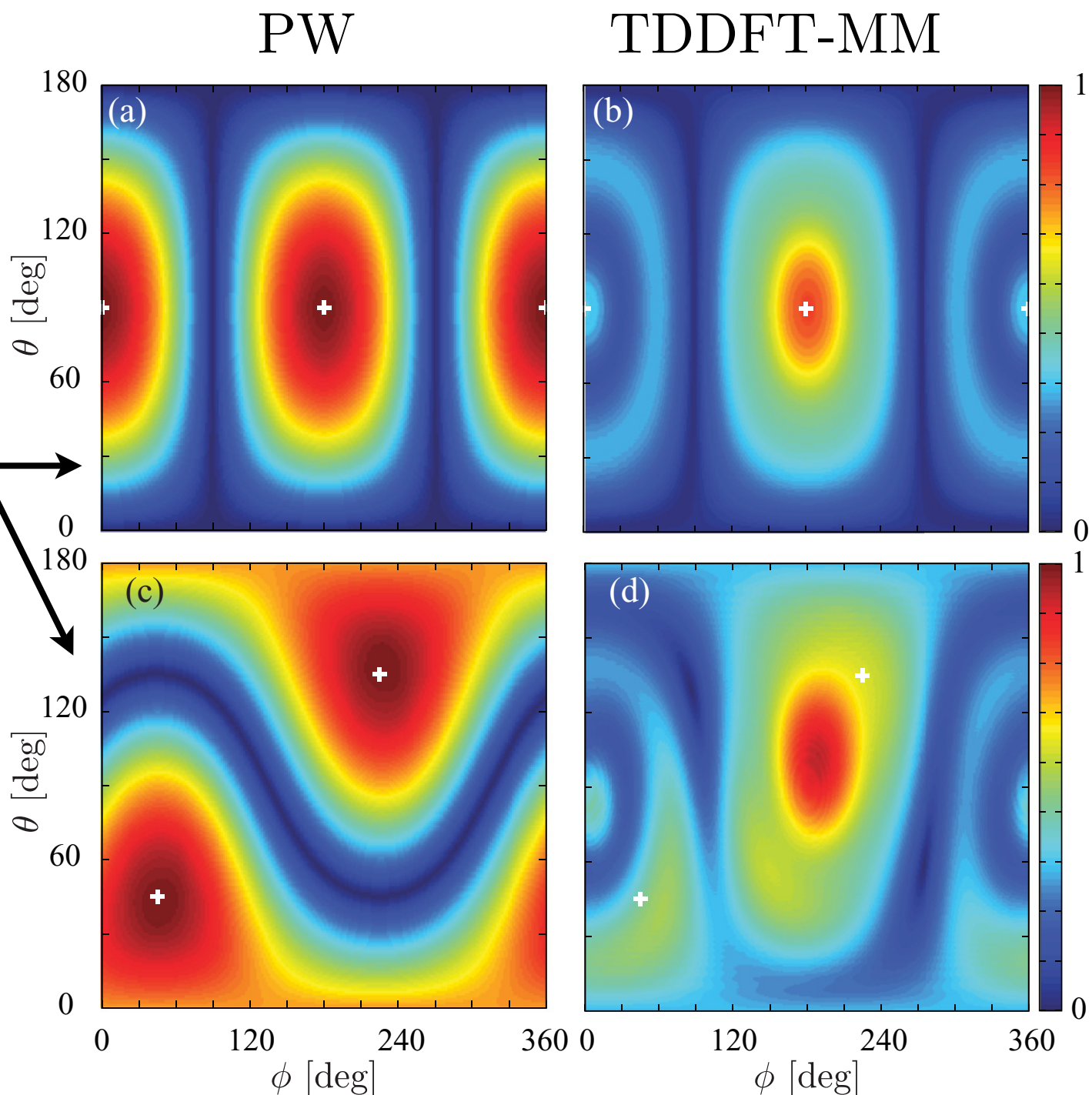
$$|\mathbf{A}_0 \cdot \mathbf{p}| \approx$$

## Remarks

- In PW angular dependence completely determined by the polarization factor
- TDDFT present asymmetry due to single atom electron emitters, maximum peaked on C atom side



HOMO  $\sigma$  symmetry



Bad agreement

# Conclusions I

Formal derivation of a **photoelectron density functional** for TDDFT from phase-space.

**Efficient** mixed real- and momentum-space **evolution scheme** based on geometrical splitting.  
MM and FMM cover a wide range of laser parameters

Observed **ATI** for H in **one-dimensional** model plus angular distributions in **3D**

PAD for randomly oriented N<sub>2</sub> molecule.

Good **agreement with experiment** (and better than SFA)

UV PAD for oriented CO and benzene: comparison **PW versus TDDFT**.

Photoelectron angular distribution carries important information on molecular orientation.

U. De Giovannini, D. Varsano, M. A. L. Marques, H. Appel, E. K. U. Gross, and A. Rubio  
*Phys. Rev. A* **85**, 062515 (2012).

# Acknowledgment

Daniele Varsano

University of Rome “La Sapienza”, Rome, (Italy)



Miguel Marques

University of Lyon and CNRS, Lyon  
(France)



Heiko Appel

Fritz-Haber-Institut, Berlin (Germany)



Hardy Gross

Max Planck Institute for Microstructure  
Physics, Halle (Germany)



Angel Rubio

University of the Basque Country, San Sebastian (Spain)



All Octopus developers

